Optimizing Ammonia Removal from Secondary Aluminum Dross as a Potential Raw Material Substitution in the Cement Industry

Prihartanto Prihartanto[1,*], Manis Yuliani[1], Wahyu Purwanta[1], Wiharja Wiharja[1], Muhammad Hanif[1], Naufal Riadhi Yusuf[1], Nida Sopiah[1], Priska Alfatri Hendrayanto[1], Sophia Shanti Meilani[2]

[1]Research Center for Environmental and Clean Technologies, National Research and Innovation Agency, Tangerang Selatan, Indonesia

[2]Environmental Engineering Department, Universitas Bhayangkara Jakarta Raya, Bekasi, Indonesia

Received 07 June 2025; received in revised form 16 October 2025; accepted 22 October 2025

DOI: https://doi.org/10.46604/ijeti.2025.15247

Abstract

Secondary aluminum dross (SAD), produced by small and medium-sized enterprises in Jombang Regency, Indonesia, is a hazardous waste with high ammonia content that threatens the environment and human health. Although SAD has potential as an alumina source for cement production, ammonia emissions restrict its safe use. This study applies a simultaneous heat-stirred alkaline leaching method to optimize ammonia removal for use as raw material in cement manufacturing. It addresses gaps in single-factor studies by optimizing multiple factors (NaOH concentration, temperature, reaction time, and stirring speed) using the Box–Behnken Design within Response Surface Methodology. Temperature and reaction time are the most influential, while interactions between NaOH and temperature, and between temperature and stirring speed, are critical for maximizing removal. The optimized process removed 98.81% ammonia, while an alternative yielded 98.34% with lower chemical and energy inputs. It enables safe SAD reuse and promotes the circular economy through waste valorization.

Keywords: alkaline leaching, ammonia removal, cement industry, secondary aluminum dross

1. Introduction

Aluminum is essential in modern industry due to its strength-to-weight ratio, lightness, corrosion resistance, and flexibility [1]. Since the 1950s, global demand has risen due to industrialization, population growth, and improved living standards [2]. About 75% of aluminum is consumed by the transportation, construction, packaging, and electrical sectors, with demand expected to increase 40% from 86.20 to 119.50 million tons between 2020 and 2030. This trend contributed to the growth of primary aluminum (PA) production from 24.66 to 73.01 million tons between 2000 and 2022 [3]. The other study reported that the worldwide growth increased from 52.29 to 70.79 million tons between 2013 and 2023, while recycled aluminum rose from 24.33 to 38.73 million tons [4]. The rise in PA output has raised concerns over resource depletion and CO_2 emissions (6.70–16.50 tons per ton) in regions like the US and Europe [5]. Consequently, emphasis has shifted toward secondary aluminum (SA) production, which consumes only 5–15% of the energy required for primary aluminum (PA) production and substantially reduces greenhouse gas emissions [6-7].

PA production generally begins with refining bauxite into alumina via the Bayer process, followed by the Hall–Héroult method to produce metallic aluminum, which generates dross as a byproduct. However, several methods are applied to recover secondary aluminum (SA) from aluminum scrap, including the Hoopes process, gas fluxing, filtration, and salt cake treatment

* Corresponding author. E-mail address: prih001@brin.go.id

[8]. High-temperature plasma smelting has also proven effective for decomposing aluminum oxides, although it requires substantial energy input [9]. Further approaches for alumina recovery from SA have also been investigated, such as precipitation, hydrometallurgy (acid and alkaline leaching), sol-gel processing, and hydrothermal methods [4, 10].

Among the available recycling methods, remelting of SA with salt flux is the most commonly employed technique [11]. In this process, SA is melted at approximately 800 °C to remove impurities, produce a pure aluminum cast, and then cooled into ingots or billets. Additionally, household aluminum waste undergoes pre-treatment through thermal de-coating, solidification, and sizing before remelting [8]. Secondary aluminum dross (SAD) forms when molten aluminum reacts with oxygen in the air, resulting in an alumina surface layer (Al_2O_3). Besides alumina, SAD primarily consists of aluminum nitride (AlN), aluminum carbide (Al_3C_3), silicon oxide (SiO_2), metallic aluminum, chlorine salts, fluorine salts, and trace amounts of silicon, iron, and magnesium. Previous studies have shown that SAD contains 40–60 wt% Al_2O_3, 2–5 wt% metallic Al, 5–30 wt% AlN, 5–15 wt% salts, 3–10 wt% heavy metal oxides, and other minor components [4]. AlN is formed through a reaction between aluminum and nitrogen gas introduced during high-temperature refining [12]. SAD may also contain sodium, nitrogen, potassium, chlorine, fluorine, and trace amounts of titanium, sulfur, manganese, and vanadium [13].

Due to its high Al_2O_3 content, SAD has potential as an alternative alumina source for clinker production, comparable to high-alumina bauxite usually used in the cement industry. This substitution could reduce production costs and conserve natural resources. SAD is particularly suitable for aluminate and sulfoaluminate cement, which require high Al_2O_3 levels, rather than ordinary Portland cement. However, the presence of AlN poses a significant challenge. When exposed to moisture, AlN undergoes hydrolysis, releasing ammonia gas, a toxic, flammable, and potentially explosive substance [4, 6]. Ammonia emissions adversely affect cement properties and pose serious health hazards, including skin burns, respiratory damage, and, at high concentrations, even death. Therefore, in the cement industry, the high ammonia content in SAD represents a primary health risk to workers during handling and processing.

This issue is especially critical in Jombang Regency, East Java, Indonesia, where over 86,458.90 tons of SAD were illegally disposed of at more than 100 locations in 2024 [14]. Although local cement producers are interested in utilizing SAD as a raw material due to its high alumina content, concerns over ammonia emissions and their implications for cement quality and occupational safety have led to prudent consideration. Therefore, effective pre-treatment methods to neutralize AlN and reduce ammonia release are essential before SAD can be applied safely in cement production. Hydrometallurgical or pyrometallurgical methods can reduce AlN content in SAD [15-16]. Hydrometallurgical methods—such as leaching and solid-liquid separation—are preferred due to their lower energy use. In contrast, pyrometallurgical methods, including calcination and sintering, heat materials to 500–1000 °C, effectively convert AlN to alumina (Al_2O_3) but consume significantly more energy.

Improving AlN removal efficiency remains a key challenge in the hydrometallurgical treatment of SAD. Previous studies have shown that factors such as temperature, reaction time, particle size, stirring speed, pressure, and alkaline additives significantly influence AlN hydrolysis, while the liquid-to-solids (L/S) ratio has a minor impact. Optimum conditions (95 °C, 180 min, L/S ratio 6 mL/g, 4 wt% NaOH) reached 96.24% removal efficiency. Pre-treatment with Wet-Stirred milling followed by alkaline leaching further increased efficiency to 98.30% [17].

In addition to alkaline leaching, AlN can also be removed by water leaching, acid leaching (using HCl or H_2SO_4), or oxidation processes (using H_2O_2 or O_3) [18-19]. Acid leaching produces aluminum sulfate and aluminum chloride, compounds that are more compatible with cement production [4]. Conversely, alkaline leaching is primarily employed to obtain a purer aluminate solution, as it generates sodium aluminate, a compound suitable for alumina production. Numerous studies have demonstrated that NaOH is highly effective in removing AlN. Therefore, this study utilized alkaline leaching with NaOH as the preferred method to reduce ammonia content in SAD.

Previous studies have shown that alkaline concentration, temperature, reaction time, and stirring speed affect the efficiency of ammonia removal from SAD. However, most research focused on single-factor effects while keeping other variables constant. These studies did not evaluate the combined interactions of these variables [13, 17]. Consequently, the simultaneous influence of these parameters remains unclear. To address this gap, the present study introduces a heat-stirred alkaline leaching method. The Box–Behnken Design within the Response Surface Methodology framework is used to optimize this method. This method systematically evaluates the simultaneous effects of NaOH concentration, temperature, reaction time, and stirring speed. Multi-factor optimization generates a predictive model for enhanced ammonia removal, providing a comprehensive understanding of how variables interact. As a result, chemical and energy consumption are reduced. The novelty of this study lies in integrating a simultaneous heat-stirred alkaline leaching system with statistical multi-factor optimization. By developing a predictive and efficient ammonia removal process, this integration enables the safe and sustainable repurposing of SAD as an alternative Al_2O_3 source in cement production.

2. Methods and Materials

The methods and materials include outlining the study area of aluminum dross (AD) recycling in Jombang Regency to provide contextual background for the study. It also describes the sampling method, preparation, and characterization of SAD to evaluate its recycling potential and associated risks. Experiments were conducted to optimize ammonia removal under various process conditions, as detailed in the following subsections.

2.1. Study area description

The recycling businesses for AD in Jombang Regency, East Java, Indonesia, are dispersed across 20 villages in the Sumobito and Kesamben Districts rather than concentrated in a single industrial zone. Fig. 1 shows the two regencies, covering 47.64 km^2 and 51.72 km^2, respectively, based on the administrative boundary map provided by the Geospatial Information Agency of Indonesia [18]. Across these regencies, at least 136 recycling industries—ranging from small to large scale—are currently operating. Small and medium-sized enterprises (SMEs), many of which operate informally and under suboptimal environmental conditions, constitute the majority of these businesses. Therefore, the study site focuses on both regencies, taking into account these conditions.

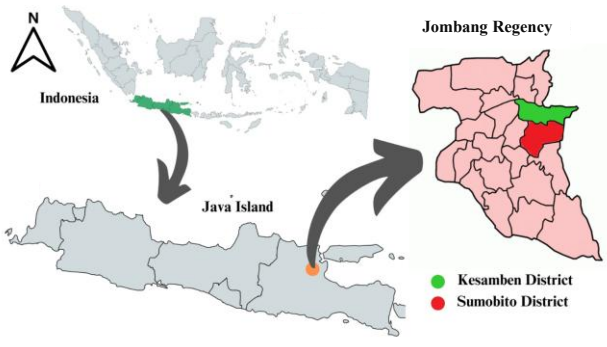

Fig. 1 Study area description

In Jombang Regency, both large- and small-scale SMEs are involved in AD recycling, employing varying technological sophistication. Fig. 2 shows the typical cascade of the AD recycling process at both SME scales. Approximately ten large-scale modern SMEs in Jombang, each with a maximum production capacity of 7 tons per day, possess advanced AD recycling technology and operate within a well-structured formal business framework. The modern recycling begins with sorting PAD to remove impurities, followed by grinding and sieving to homogenize the material. The refined material is then processed in a furnace, producing aluminum ingots and SAD. These processes convert PAD into aluminum ingots and SAD, with an average ingot-to-SAD production ratio of 60:40.

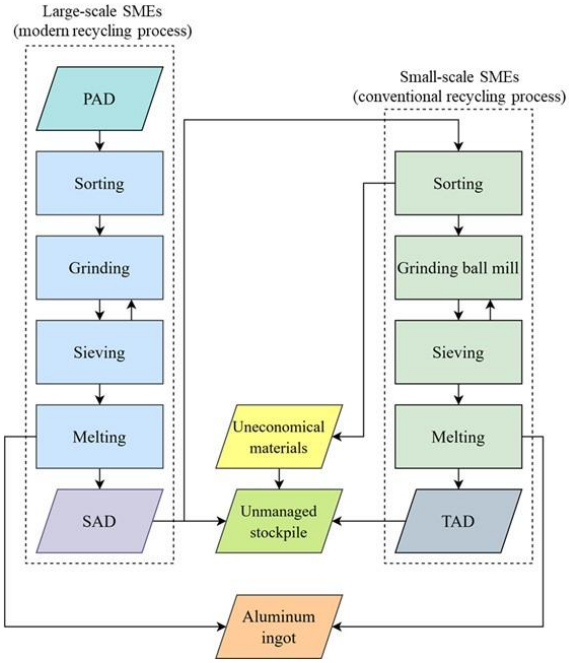

Fig. 2 The typical cascade of the AD recycling process at a large-scale and a small-scale SME

The SAD is recycled using conventional technology by small-scale SMEs, each with a maximum production capacity of 1.50 tons per day. This secondary process yields 16% aluminum ingots and 84% tertiary AD (TAD). TAD is a by-product composed of aluminum oxides, salts, and impurities formed during recycling and refining, particularly after primary and secondary dross processing on the surface of molten aluminum. It represents a more advanced stage in the recycling cycle, resulting in a more complex mixture derived from the by-products of earlier dross treatment stages.

2.2. SAD and SEM-EDX characteristic analysis

This study examines the crystalline phase composition of SAD and elemental composition to evaluate its recycling potential and risks to human health. The crystalline phase was analyzed using X-ray diffraction (XRD) with a Rigaku SmartLab diffractometer (Cu Kα, λ = 1.5406 Å). The SAD sample was refined into powder using a sieve with 200 mesh (≤75 μm) and dried at 110 °C for 2 hours to remove moisture. A 0.50–1.00 g powder sample was placed in a back-loaded holder to minimize preferred orientation effects. For optimal resolution, X-ray diffraction (XRD) data were collected over a 2θ range of 10°–90° with a step size of 0.01°, at a scanning rate of 5°/min, using an operating voltage of 40 kV and a current of 30 mA. Phase identification was analyzed using Rigaku PDXL software by comparing diffraction patterns with the ICDD database.

Surface morphology and elemental composition were analyzed using Scanning Electron Microscope-Energy-Dispersive X-ray (SEM-EDX) JEOL JSM-IT200. A 0.50–1.00 g powder sample was coated with carbon using a sputter coater to enhance conductivity and minimize charging effects. The sample was mounted on a conductive holder and imaged under high-vacuum conditions using an accelerating voltage of 15 kV. For energy-dispersive X-ray (EDX) analysis, a specific area of interest was selected, and then high-energy electron beams were applied to excite the emission of characteristic X-rays. These X-rays were used to generate an elemental spectrum and distribution map. Elemental quantification was carried out using ZAF correction to compensate for atomic number (Z), absorption (A), and fluorescence (F) effects.

2.3. Analytical test and optimization methods

SAD samples were collected from aluminum recycling SMEs in Sumobito and Kesamben Districts, Jombang Regency, East Java, Indonesia, between January and March 2024. At least 1 kg of each sample was randomly taken from stockpiles before use as raw material in conventional AD recycling processes by small-scale SMEs. The samples were homogenized and

sealed in polyethylene containers for transfer to the laboratory, where they underwent alkaline leaching experiments to optimize the efficiency of ammonia removal. To identify the optimum process parameters affecting ammonia removal from SAD, a statistical approach was employed using the Box-Behnken Design (BBD) method, integrated with Response Surface Methodology (RSM), in Design-Expert software (version 13). This method was chosen for its efficiency in modeling second-order (quadratic) effects, minimizing the number of experimental runs, and avoiding extreme factor combinations that could be undesirable due to safety or operational feasibility concerns.

Four independent variables (temperature (B), reaction time (C), stirring speed (D), and NaOH concentration (A)) were optimized using RSM [19]. These parameters were selected because previous studies identified them as key factors in AlN hydrolysis and ammonia release from SAD [13, 17, 19]. NaOH controls alkalinity and AlN solubility; high concentrations promote ammonia release, but excessive amounts may produce adverse effects or saturation [13]. Temperature enhances reaction kinetics and ammonia volatilization, making it the primary factor [9]. Reaction time controls hydrolysis extent and equilibrium; sufficient time ensures complete AlN decomposition, but excessive time may limit efficiency [17]. Mass transfer is controlled by the speed of stirring; appropriate agitation increases mixing, but excessive churning provides little benefit [19].

The BBD was selected for this study because of its practical advantages over other methods. Unlike CCD, which includes axial (star) points at extreme factor values that may expand the design space but are impractical, unsafe, or challenging to implement, BBD avoids such extremes by placing runs in the middle of factor ranges and at the center point. This makes the design safer while also allowing for accurate assessment of quadratic and interaction effects. In this study, the BBD center points were replicated three times to estimate pure error and conduct lack-of-fit tests. The robustness, sufficiency, and accuracy of the model were demonstrated through error analysis, which included pure error variance, R^2, adjusted R^2, predicted R^2, and adequate precision. Compared to CCD, BBD achieves reliable error estimation with fewer experimental runs and avoids the variability introduced by extreme factor levels. Overall, BBD was preferred for its combination of safety, efficiency, and statistical reliability, providing sufficient replicates and error analysis without the challenges associated with extreme factor levels [20].

The experiment involved simultaneously analyzing the effects of variations in NaOH concentration (0, 3.50, 7 wt%), temperature (25, 60, 95 ^oC), reaction time (30, 135, 240 minutes), and stirring speed (0, 200, 400 rpm) on ammonia removal efficiency (Table 1). The selection of experimental parameters was based on findings from previous studies to ensure that the tested ranges were both relevant and reliable. The upper limits were based on the highest effective values reported from previous studies. These values were NaOH concentrations of up to 7 wt% (4 wt% [21]; 5 wt% [17]; 7 wt% [22]); temperatures of up to 95 °C (75 ^oC [17]; 95 ^oC [21, 22]); reaction times of up to 240 minutes (120 min [17]; 180 min [21]; 240 min [22]); and stirring speeds of up to 400 rpm [22]. In contrast, the lower limits were set as simple baseline conditions: no NaOH addition (0 wt%), room temperature (25 °C), no stirring (0 rpm), and a short reaction time of 30 minutes, as adopted in previous studies [23]. These upper and lower values were then applied in the BBD, which produced the experimental combinations: NaOH concentrations of 0, 3.50, and 7 wt%; temperatures of 25, 60, and 95 °C; stirring speeds of 0, 200, and 400 rpm; and reaction times of 30, 135, and 240 minutes.

Table 1 The coding of experimental factors and levels

Factors	Units	Code	Code values of different levels		
			-1	0	1
NaOH concentration	%	A	0	3.50	7
Temperature	^oC	B	25	60	95
Reaction time	minute	C	30	135	240
Stirring speed	rpm	D	0	200	400

The L/S ratio was kept constant at two throughout the experiments [17]. The BBD matrix comprised 29 experimental runs, incorporating mid- and high/low levels without corner points and replicates at the center point to estimate experimental

error. Table 1 shows the coded levels of the four independent variables examined. Each variable was evaluated at three levels: low (-1), medium (0), and high (1). This methodology allowed the evaluation of linear, quadratic, and interaction effects among variables, supporting the development of a predictive model for ammonia removal efficiency.

The significance of the model was evaluated using analysis of variance (ANOVA), and its adequacy was assessed through the coefficients of determination (R^2, adjusted R^2, and predicted R^2), along with lack-of-fit tests, to ensure reliable predictions across the design space.

The experimental procedure consisted of three main stages: leaching, distillation, and titration. In the leaching stage, 5 g of SAD was first dissolved in deionized water with an L/S ratio of 2 [17], along with additional NaOH [19], which had been pre-dissolved in deionized water. The solution was then stirred at a controlled speed using a magnetic stirrer while a thermostatic water heater maintained the temperature, and a stopwatch recorded the reaction time. The mixture was filtered after the predetermined reaction time to separate the solid and liquid phases. The solid residue was then weighed and prepared for the subsequent distillation process.

During the distillation stage, the solid residue was placed in a boiling flask and combined with a borate buffer to maintain a stable environment for the controlled release of ammonia. The pH of the mixture was then adjusted to 9.5 using either acid or base to ensure optimum ammonia extraction. After pH stabilization, the flask was connected to a distillation apparatus, with the delivery tube submerged in a boric acid solution to collect the released ammonia gas. This preliminary distillation followed the American Public Health Association (APHA), American Water Works Association (AWWA), and American Water Environment Federation (WEF) standard 4500-NH_3-B preliminary distillation step [24]. The heat was applied gradually to avoid sudden boiling and sample loss. Distillation continued until only a minimal volume of liquid remained in the flask. The collected distillate was then prepared for titration.

During the titration stage, a mixed indicator solution of methyl red and methylene blue was added to the distillate to detect the presence of ammonia by a visible color change. The titration followed the APHA, AWWA, and WEF standard 4500-NH_3-C titrimetric method [24], using standardized 0.02 N sulfuric acid calibrated with sodium carbonate (Na_2CO_3) to ensure accuracy. Titration continued until the solution turned pale lavender, indicating the endpoint. The ammonia and ammonium contents, expressed as sodium content, were calculated based on the volume of titrant used, ensuring precise quantification of sodium species in the sample. The ammonia removal efficiency (%) can be calculated by:

$$Removal\ Efficiency = \frac{C_0 - C_t}{C_0} \times 100 \quad (1)$$

where C_0 is the initial ammonia concentration before treatment, and C_t is the residual concentration after treatment at time t. Both are represented in milligrams per liter or parts per million. Comparing these figures allows us to calculate the removal efficiency, which indicates how effectively ammonia was decreased.

3. SAD Characteristics

The SAD characterization is crucial for understanding its mineralogical and elemental composition, which influences ammonia generation, leaching behavior, and potential reuse in cement production. The characteristics of SAD were examined using XRD and SEM-EDX analysis methods. These investigations identify SAD's crystalline phases, surface morphology, and elemental distribution, allowing for the development of optimal ammonia removal and valorization techniques.

3.1. XRD analysis

The XRD analysis of the SAD sample showed a complex crystalline structure consisting of several inorganic phases, such as barium sulfate ($BaSO_4$), aluminum (Al), aluminum oxide (Al_2O_3), magnesium aluminate (Al_2MgO_4), alumino-silicates,

aluminum nitride (AlN), aluminum-magnesium alloys, silica (SiO_2), and titanium oxides (Ti_3O_5), with barium sulfate having the highest intensity (Fig. 3). The detection of magnesium aluminate, aluminum, and aluminum oxide are indicating significant thermal oxidation and alloying reactions that occur during high-temperature processing. However, the presence of silica and alumino-silicates may be due to contamination by silicate-based materials, such as sand or clay, during the smelting process. Additionally, detecting AlN and titanium oxides indicates the influence of specific industrial residues [8].

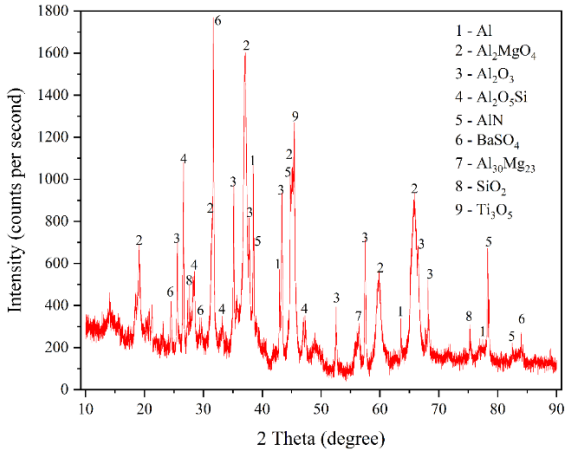

Fig. 3 XRD Analysis of SAD

The dominance of barium sulfate—previously unreported in most studies—alongside aluminum nitride, aluminum oxide, and magnesium aluminate reflects high-temperature oxidation processes and interactions between aluminum and magnesium during smelting. In addition, the presence of aluminum-magnesium intermetallics such as $Al_{30}Mg_{23}$ and titanium oxides suggests the influence of specific industrial inputs, likely from residual metals or additives introduced during earlier processing stages. While earlier studies identified aluminum oxide, aluminum nitride, silica, and magnesium aluminate as key components of SAD [4], the unusually high concentration of barium sulfate observed in this study indicates localized compositional variation, likely due to the use of barium-containing fluxes or contamination from raw materials such as clay or soil—factors commonly associated with small-scale, less-controlled recycling operations like those in Jombang Regency. Overall, the XRD analysis highlights the need for site-specific ammonia removal strategies and supports the feasibility of SAD reuse in cement applications, particularly when adapted to site-specific mineralogical profiles.

3.2. SEM EDX analysis

This study employs SEM-EDX analysis to gain a deeper understanding of the surface morphology, particle characteristics, and elemental distribution in SAD.

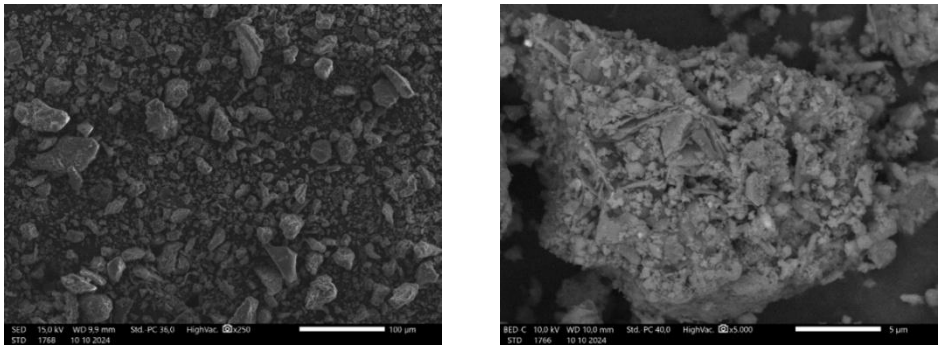

(a) 250x magnification (b) 5000x magnification

Fig. 4 SEM images of the SAD sample

Fig. 4 shows the SEM images of the SAD at different magnifications. At a lower magnification (Fig. 4(a)), the size distribution of the SAD particles is heterogeneous, resulting in irregular agglomerates. It is suggested that the SAD is primarily

composed of mechanically fragmented phases rather than spherical particles, which are usually generated by melting or sintering, as the surface morphology shows the presence of angular and sharp-edged particles. Small particles can adhere to the surface of larger fragments due to the relative porosity of the microstructure. At higher magnification (Fig. 4(b)), a more complex texture is observed with fine particles dispersed throughout the layered and laminated formation.

Table 2 presents the elemental composition of the SAD sample, analyzed using the SEM-EDX method at eight different points. The results show that oxygen and aluminum are the predominant elements, with average concentrations of 43.05% and 33.98%, respectively. However, most of the aluminum is likely present in the form of aluminum oxide. In addition to these elements, barium also appears at a relatively high concentration, although it was only detected at point 1. This finding suggests that barium is not uniformly distributed and is most likely present as localized particles, such as barium sulfate [25].

Compared to previous studies, the aluminum content (33.98%) in this sample is slightly lower than the reported range (36.08–51.84%), while the oxygen content (43.05%) falls within the expected range (23.40–45.00%) [5]. Additionally, the concentrations of magnesium (3.93%) and sodium (1.96%) are consistent with earlier findings, whereas the titanium level (1.14%) exceeds the commonly reported range (0.11–0.32%) [5]. The exceptionally high barium content (61.34%) was not reported in previous studies, suggesting the presence of localized barium sulfate, as further evidenced by the accompanying sulfur content (1.36%). Trace elements such as carbon and sodium were found in lower concentrations than earlier reports, indicating a reduced presence of organic matter or contamination in this sample [6].

Table 2 Elemental composition of the SAD

Element	Mass percentage (%)							
	Point 1	Point 2	Point 3	Point 4	Point 5	Point 6	Point 7	Point 8
Carbon	–	2.88±0.06	–	–	–	–	–	10.24±0.28
Nitrogen	ND	0.14±0.05	ND	10.56±0.14	ND	ND	ND	0.76±0.13
Oxygen	19.23±0.18	47.02±0.29	52.78±0.28	34.58±0.25	51.15±0.29	51.38±0.26	55.11±0.28	33.16±0.51
Fluor	–	–	–	4.26±0.12	–	–	–	–
Sodium	–	2.93±0.09	–	2.55±0.08	3.73±0.11	2.95±0.08	–	3.53±0.19
Magnesium	–	8.09±0.14	5.45±0.12	2.75±0.09		4.06±0.09	7.90±0.13	3.21±0.19
Aluminum	8.58±0.18	29.71±0.28	41.77±0.33	43.54±0.32	45.11±0.35	34.71±0.27	30.72±0.27	37.70±0.62
Silica	–	–	–	–	–	1.01±0.07	–	–
Potassium	–	–	–	1.22±0.11	–	0.65±0.08	–	–
Chloride	–	1.77±0.10	–	–	–	1.09±0.07	–	11.41±0.46
Calcium	–	0.73±0.10	–	0.55±0.09	–	1.76±0.12	6.26±0.21	–
Titanium	–	6.74±0.30	–	–	–	2.39±0.17	–	–
Sulfur	10.85±0.22	–	–	–	–	–	–	–
Barium	61.34±1.23	–	–	–	–	–	–	–

ND: not detected

Several minor elements, including magnesium (3.93%), sodium (1.96%), titanium (1.14%), sulfur (1.36%), carbon (1.64%), and nitrogen (1.43%), were also detected. The presence of magnesium, sodium, and titanium is likely due to contamination or additives introduced during earlier processing stages. Sulfur is presumed to be associated with barium in the form of barium sulfate. Carbon likely originates from residual organic matter or combustion by-products. Sodium, like the other minor elements, was detected only at specific points (2, 4, and 8), suggesting uneven distribution and possible localized contamination [8-9].

These findings highlight the variability in SAD composition, which depends on its origin and refining process. The notable presence of aluminum oxide and barium sulfate supports the potential application of SAD in cement manufacturing. Aluminum oxide contributes to the formation of calcium aluminate cement (CAC), which is advantageous for high-temperature applications [6]. Meanwhile, barium sulfate may act as a mineralizer, enhancing the performance, workability, and energy efficiency of cement during production [25]. Utilizing SAD in cement production offers a sustainable approach to waste management, helping reduce the environmental impact of both the aluminum and cement industries. With appropriate processing, SAD can potentially serve as an eco-friendly material for construction.

4. Results

The BBD method, as part of RSM, was used to generate key data and assess the factors affecting ammonia removal from SAD. RSM was then applied to develop predictive models and analyze variable effects. The following subsections present regression analysis, ANOVA, and interaction effects among the factors to demonstrate the optimized process performance.

4.1. Regression model and ANOVA analysis

The ammonia removal efficiencies measured across this set of experiments ranged from 9.51% to 98.05%, resulting from BBD matrix experimental runs. Given this range of values, a quadratic regression model was developed using the BBD data to describe the relationship between process factors and ammonia removal efficiency, using a logit transformation, which is presented as:

$$Logit\,(Ammonia\ Removal) = ln(Ammonia\ Removal) / (100 - Ammonia\ Removal)] = 1.54 + 0.17A + 1.94B + 0.57C - 0.28D + 0.55AB + 0.05AC - 0.15AD + 0.26BC + 0.89BD - 0.24CD - 0.45A^2 - 0.23B^2 - 0.25C^2 + 0.19D^2 \quad (2)$$

Table 3 ANOVA results for the quadratic regression model of ammonia removal efficiency

Source	Sum of squares	dF	Mean square	F-value	p-value	Significance	Effect on efficiency
Model	57.54	14	4.11	17.82	< 0.0001	significant	Model is statistically significant and robust
A-NaOH concentration	0.34	1	0.34	1.46	0.2463	not significant	Increasing NaOH concentration beyond optimum had little effect
B-temperature	45.14	1	45.14	195.75	< 0.0001	significant	Higher temperature accelerates AlN hydrolysis and ammonia removal
C-reaction time	3.84	1	3.84	16.63	0.0011	significant	Reaction time moderately improves removal efficiency
D-stirring speed	0.95	1	0.95	4.10	0.0623	not significant	Extra agitation did not notably enhance efficiency
AB	1.23	1	1.23	5.32	0.0368	significant	NaOH more effective at higher temperature.
AC	0.01	1	0.01	0.04	0.8360	not significant	Optimum NaOH reached, extended reaction time gave no benefit
AD	0.09	1	0.09	0.38	0.5474	not significant	Increased agitation gave no additional benefit
BC	0.27	1	0.27	1.18	0.2955	not significant	Higher temperature slightly improved efficiency
BD	3.16	1	3.16	13.69	0.0024	significant	Combined high temperature and stirring speed enhance removal
CD	0.23	1	0.23	0.99	0.3352	not significant	Dominant effect from reaction time, while stirring effect minimal
A^2	1.31	1	1.31	5.69	0.0317	significant	Non-linear effect at excessive NaOH due to saturation or side reactions.
B^2	0.33	1	0.33	1.43	0.2514	not significant	Linear effect
C^2	0.39	1	0.39	1.69	0.2144	not significant	Linear effect
D^2	0.24	1	0.24	1.05	0.3222	not significant	Linear effect
Residual	3.23	14	0.23	–	–	–	–
Lack-of-fit	2.79	10	0.28	2.53	0.1924	not significant	–
Pure error	0.44	4	0.11	–	–	–	–
Cor total	60.77	28	–	–	–	–	–

ANOVA was performed to evaluate the significance of each factor and its interaction in this model by assessing the p-value (<0.05) for relevance, F-value for model fit, and R^2 for predictive performance. The ANOVA analysis evaluates the impact of NaOH concentration (A), process temperature (B), reaction time (C), and stirring speed (D), as well as their

interaction on ammonia removal efficiency (Table 3). The model is highly significant ($F = 17.82$, $p < 0.0001$), explaining most data variability. The model sum of squares (57.54 out of a total of 60.77) confirms its robustness in predicting ammonia removal efficiency, making it a reliable tool for optimization.

4.2. Effect of individual factor

According to Table 3, NaOH concentration (A) did not significantly affect ammonia removal efficiency ($F = 1.46$, $p = 0.2463$), indicating that increasing alkalinity beyond a certain threshold did not substantially enhance ammonia removal, likely due to saturation effects [13]. In contrast, process temperature (B) was the most significant factor ($F = 195.75$, $p < 0.0001$), consistent with previous studies [9, 11], as higher temperatures improve reaction kinetics, enhance mass transfer, and increase the solubility of reactants, accelerating AlN hydrolysis, as in the following reaction [4]:

$$AlN(s) + 3H_2O\ (l) + NaOH\ (aq) \rightarrow Na[Al(OH)_4] + NH_3(g) \quad (3)$$

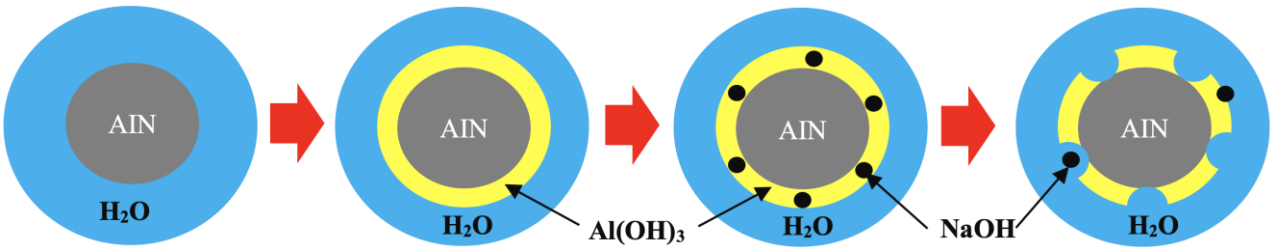

Fig. 5 AlN hydrolysis with NaOH added in SAD

As shown in Fig. 5, alkaline hydrolysis of AlN occurs when it reacts with water and NaOH, producing soluble sodium aluminate and ammonia gas. AlN hydrolyzes to aluminum hydroxide and NH_3, then dissolves in an alkaline medium. Scrubbers or acid absorption are used to collect released NH_3 and avoid emissions. This allows for safe reuse of SAD in industrial applications. At low temperatures, a protective layer slows hydrolysis, but at higher temperatures, the reaction shifts from diffusion-controlled to surface- and product-layer-controlled, lowering activation energy and accelerating removal [9]. Reaction time (C) also significantly affected performance ($F = 16.63$, $p = 0.0011$), as longer durations allow for more complete degradation or adsorption of ammonia. Furthermore, stirring speed (D) had no impact ($F = 4.10$, $p = 0.0623$), and NaOH concentration (A) didn't matter either ($F = 1.46$, $p = 0.2463$), indicating that adding more agitation or making the solution more alkaline didn't help remove ammonia because of saturation effects [13]. Therefore, temperature and reaction time were the most crucial factors in determining process efficiency, whereas stirring speed and NaOH concentration had a minimal effect.

4.3. Interaction effects between factors

While individual factor analysis reveals major influences on ammonia removal, interaction effects reveal how factor pairs jointly impact the response. This study analyzes six interactions of factors that affect ammonia removal efficiency, which are summarized in Table 3 and illustrated in Fig. 6 with a 3D response surface graph.

The results showed that the interaction effect between process variables significantly affected the ammonia removal efficiency. As summarized in Table 3, the NaOH concentration and temperature interaction (AB) significantly influenced ammonia removal efficiency at a fixed reaction time of 135 minutes and a stirring speed of 200 rpm ($F = 5.32$, $p = 0.0368$), indicating that NaOH efficacy is temperature-dependent [13]. High temperatures enhanced solubility and reaction kinetics, resulting in a maximum effectiveness of 97.23% at 95 °C and 6.50 wt% NaOH (Fig. 6(a)). However, NaOH alone showed no significant significance ($p = 0.2463$), possibly due to saturation effects. Excessive NaOH raises the hydrolysis pH, shifting the AlN balance toward reactants and limiting breakdown. AlO_2^- precipitates as $Al(OH)_3$, possibly blocking hydrolysis [9, 13].

This study found that increasing temperatures improved ammonia removal efficiency despite high OH^- concentrations. Thus, the interaction between temperature and NaOH concentration distinguishes these results from earlier findings, highlighting temperature as a key factor in enhancing ammonia removal.

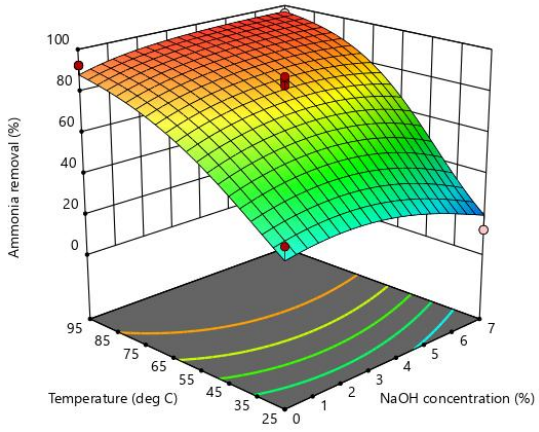

(a) Interaction between NaOH concentration and temperature

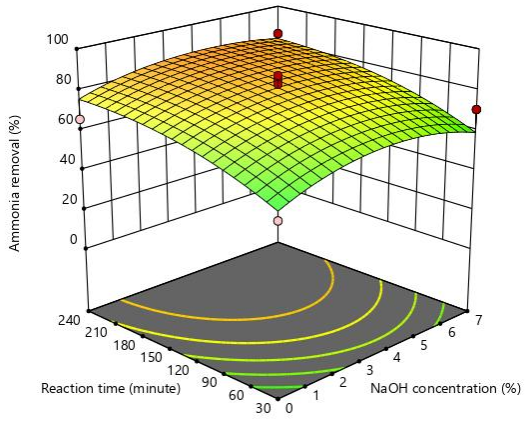

(b) Interaction between NaOH concentration and reaction time

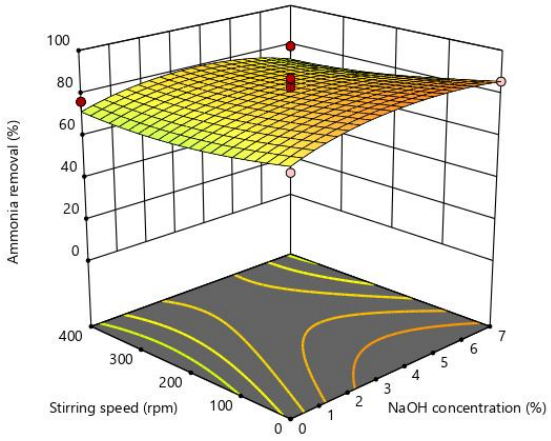

(c) Interaction between NaOH concentration and stirring speed

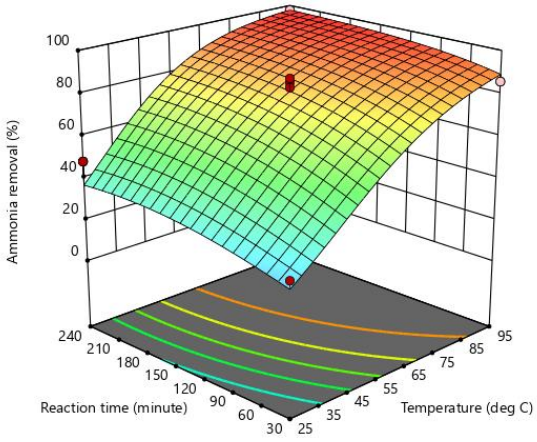

(d) Interaction between reaction time and temperature

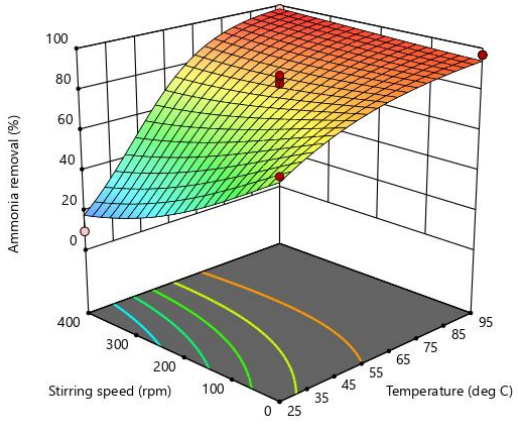

(e) Interaction between stirring speed and temperature

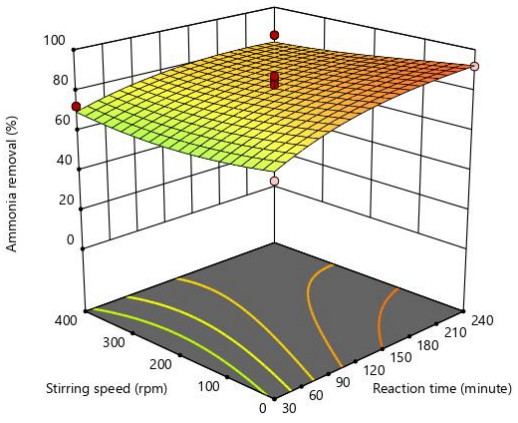

(f) Interaction between stirring speed and reaction time

Fig. 6 3D response surface of factor interactions affecting ammonia removal

Besides the (AB) interaction, the interaction between temperature and stirring speed (BD) was also statistically significant ($F = 13.69$, $p = 0.0024$), indicating that better mixing enhanced heat distribution and reactant contact. As shown in Fig. 6(e), removal efficiency increased with both factors, reaching a maximum of 98.11% at 95 °C and 400 rpm and a minimum of 17.14% at 25 °C and 400 rpm, with a constant reaction time of 135 minutes and NaOH concentration of 3.50 wt%.

The interactions between NaOH concentration and reaction time (AC, F = 0.04, p = 0.8360), NaOH concentration and stirring speed (AD, F = 0.38, p = 0.5474), temperature and reaction time (BC, F = 1.18, p = 0.2955), and reaction time and stirring speed (CD, F = 0.99, p = 0.3352) were all statistically insignificant, indicating a minimal synergistic effect on ammonia removal efficiency. As shown in Fig. 6(b) for (AC), once the NaOH concentration reached its optimum level, increasing the reaction time provided no additional benefit because of diffusion limits and the formation of a particle surface layer [13]. Increased agitation did not improve NaOH performance in (AD), with a maximum efficiency of 88.80% at 0 rpm and 4.50 wt% NaOH at 60°C for 135 min (Fig. 6(c)). For (BC), extended reaction time had a minimum effect at lower temperatures, but higher temperatures improved efficiency due to the primary effect of temperature, reaching 97.31% at 95°C and 240 min at 3.50 wt% NaOH and 200 rpm (Fig. 6(d)). For (CD), ammonia removal was dominated by reaction time (p = 0.0011), with limited stirring effect, reaching 93.00% at 240 min and 0 rpm (Fig. 6(f)).

Following the overall model significance, the effects of individual terms, particularly the quadratic components, were further analyzed. NaOH concentration (A^2) showed a significant non-linear impact (F = 5.69, p = 0.0317), indicating diminishing returns likely due to saturation or side reactions at higher concentrations. In contrast, temperature (B^2), reaction time (C^2), and stirring speed (D^2) did not show significant quadratic effects (p > 0.05), indicating that their impacts could be described as linear within the experimental domain.

The model analysis indicates that the interaction between NaOH concentration and temperature significantly influences ammonia removal efficiency, with an R^2 of 0.9469, adjusted R^2 of 0.8937, and predicted R^2 of 0.7244. The model's robustness and predictive capability for process optimization are confirmed by a sufficient precision value of 16.38, well above the threshold of 4, indicating a strong signal-to-noise ratio. These findings underscore the significance of targeted interaction effects in enhancing process performance and suggest that further increases in NaOH concentration may yield limited benefits due to saturation phenomena [11]. The validated model provides a practical basis to guide future optimization of ammonia removal processes.

5. Discussion

This discussion investigates which operating conditions and interactions of key factors most affect ammonia removal from SAD. Along with maximizing removal efficiency, the process is assessed for feasibility, sustainability, and safety. The findings further suggest how SAD may help the cement industry achieve circular economy and resource efficiency goals.

5.1. Ammonia removal optimization

The experimental results generated by Design Expert, which had the highest desirability score (1.000), are ranked from highest to lowest in ammonia removal efficiency, as shown in Table A1 of the supplementary data in the appendix. The best-performing condition achieved an efficiency of 98.81% at 5.30 wt% NaOH concentration, a temperature of 94.19 °C, a reaction time of 239.49 minutes, a stirring speed of 398.49 rpm, and an L/S ratio of 2. While this condition represents the technological maximum, it requires a relatively large alkali dose, which may increase both operational expenses and environmental impact. To identify a more practical and sustainable alternative, an optimum condition is selected from the top-performing findings using the lowest NaOH content. With 2.90 wt% NaOH concentration (Fig. (7a)), 94.22 °C temperature (Fig. (7b)), 217.62 minutes reaction time (Fig. (7c)), and 399.70 rpm stirring speed (Fig. (7d)), while maintaining the same L/S ratio, as illustrated in the desirability profile (Fig. (7e)), the process achieved a slightly lower removal efficiency of 98.34%. Although not the absolute highest, this condition balances performance, cost, and environmental impact.

Temperature is the most significant factor affecting ammonia removal efficiency, with a high positive correlation to performance, as analyzed by ANOVA. Additionally, reaction time had a considerable effect, highlighting its critical role in

the process and emphasizing the importance of evaluating combinations of these factors throughout the optimization [6, 10]. Notable interaction effects, particularly between temperature and reaction time (p = 0.0024), underscore the importance of integrating these variables. Reducing reaction time to 135 minutes will lead to significant trade-offs. Although it may reduce processing time, it requires a higher NaOH concentration (3.50%) and an elevated temperature (95 °C) to achieve a lower ammonia removal efficiency (98.10%), compared to 98.34% at 217.62 minutes with reduced NaOH usage and milder thermal input. These conditions may lead to increased energy consumption, chemical usage, operational costs, and elevated safety and environmental risks associated with high temperatures and chemical inputs. These findings suggest that aggressively reducing reaction times can compromise removal efficiency and strain resource consumption and sustainability [7-8].

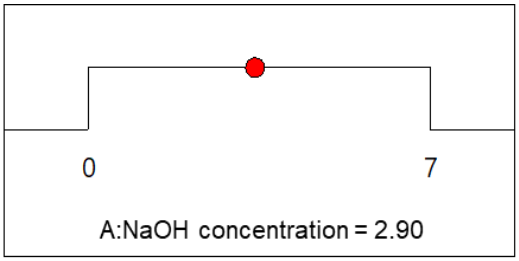

(a) Desirability ramp for NaOH concentration

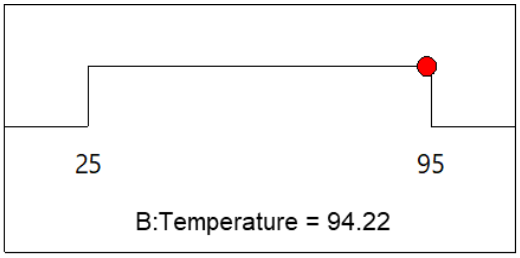

(b) Desirability ramp for temperature

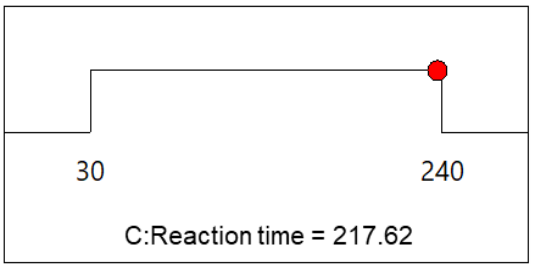

(c) Desirability ramp for reaction time

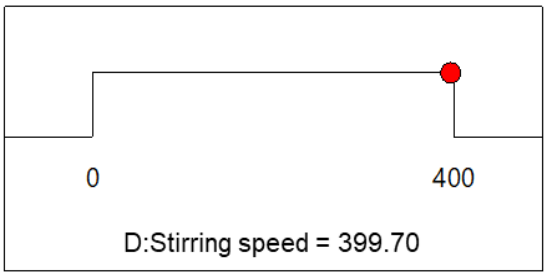

(d) Desirability ramp for stirring speed

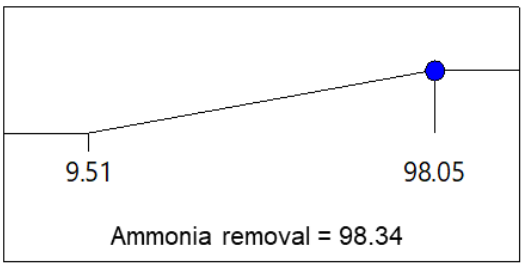

(e) Desirability ramp for ammonia removal efficiency

Fig. 7 Desirability ramps for ammonia removal optimization

Therefore, it is recommended to use a multi-objective optimization approach, which creates a balance between removal efficiency and material and energy sustainability. There are several ways to achieve this balance, such as using desirability-based optimization to identify conditions that maximize efficiency while minimizing chemical use and energy requirements and maintaining NaOH concentration and temperature within practical limits [10]. In addition, utilizing significant interaction effects, especially between temperature and reaction time, enables more efficient conditions without relying on extreme parameter values. Applying model validation, along with life cycle or environmental impact assessment, ensures that the optimized process provides technical robustness and ecological and economic viability, thus achieving sustainability goals without compromising performance [8].

These optimized conditions also demonstrate strong potential for industrial implementation. The optimum parameters (3–5 wt% NaOH, 90–95 °C, 200–240 min, 300–400 rpm, and L/S ratio 2–6) are industrially applicable and may be applied in stirred-tank or continuous leaching reactors currently used in cement plants. Alkaline wastewater, energy consumption, and ammonia emissions are major obstacles for scaling up, but they may be solved through water recycling, heat recovery, and gas

scrubbing. The lower NaOH dosage reduces chemical input and operational expenses. At the same time, the parameter ranges are consistent with existing cement plant operations, enabling safe and sustainable large-scale SAD utilization without extensive infrastructure adjustments.

5.2. Safe SAD utilization for cement production

SAD utilization in cement production presents promising prospects for enhancing product quality and promoting circular economy practices. SAD has potential as an alternative raw material, which can reduce reliance on conventional resources. However, the high ammonia content poses a significant challenge since it may negatively impact cement performance and pose serious health concerns to workers by releasing toxic gas emissions. Therefore, optimizing the ammonia removal process is essential to ensure the technical viability and environmental safety of SAD use in cement manufacturing.

This issue is particularly relevant in regions such as Jombang Regency, where several cement manufacturers are highly interested in using SAD because it is accessible locally and may benefit both the economy and the environment [6]. Nonetheless, concerns remain regarding the health and safety implications of ammonia emissions, which have limited its practical application. These uncertainties demonstrate the importance of developing a robust, efficient, and safe strategy for ammonia removal.

Ammonia removal from SAD is critical for maintaining cement quality and protecting the safety of cement manufacturing workers. A previous study found that residual ammonia can produce gypsum and ammonium salts, which extend the setting time and decrease compressive strength [26]. With an efficiency of up to 98.80%, the removal method assessed in this study mitigates these impacts while ensuring steady setting time and adequate cement hydration. This method enhances the quality and reliability of cement production while also supporting safe waste valorization.

SAD has been utilized in various types of cement, including calcium aluminate cement (CAC), ordinary Portland cement (OPC), blended cement, geopolymer cement (GC), and calcium sulfoaluminate (CSA) cement. Due to its high content of Al_2O_3, CaO, SiO_2, Fe_2O_3, and FeO, SAD is a promising alternative raw material for clinker formation and cement hydration in CAC production [6]. CAC is particularly valued for its fire-resistant properties, sulfate resistance, and rapid setting. In OPC, SAD is a supplementary cementitious material (SCM) that partially replaces clinker to enhance sulfate and chemical resistance. However, it is essential to control the levels of ammonia, chloride, and heavy metals to ensure the desired quality of the final product.

Adding SAD alongside fly ash and slag in blended cement can enhance production efficiency, reduce carbon emissions, and improve durability under harsh environmental conditions. Moreover, SAD has the potential as an alternative material for GC, a clinker-free, aluminosilicate-based cement that offers significant environmental benefits. The Al_2O_3 and SiO_2 content in SAD is particularly beneficial in GC applications, as it supports the development of a robust aluminosilicate network, which improves both mechanical strength and chemical resistance [27].

SAD also contributes to the production of CSA cement, which plays a key role in accelerating setting time, reducing energy consumption, and lowering CO_2 emissions compared to conventional Portland cement. A specific CSA clinker is synthesized using a mixture of 45.53 wt% SAD, 12.82 wt% fluorgypsum, 0.64 wt% fly ash, and 41.00 wt% $CaCO_3$. The resulting CSA cement exhibited high compressive strength, ranging from 40 to 47 MPa at 20 °C after 28 days, comparable to the 43.70 MPa strength of ordinary Portland cement [28].

Although no specific international standards regulate ammonia content in raw cement materials, its concentration remains a critical concern for the practical use of SAD as an SCM, including in the Jombang Regency. Elevated ammonia levels cause two significant issues. Firstly, the emission of ammonia gas during cement mixing poses a risk to worker health. Second, even

at low levels (above 0.04% or 400 ppm), ammonia in SAD or fly ash can degrade cement quality, reducing compressive strength and extending mortar or concrete setting times.

In Jombang, worker health risks are a major factor in evaluating SAD's viability. A significant concern is the release of toxic, flammable, and explosive gases, such as CH_4, NH_3, PH_3, H_2, and H_2S when SAD reacts with moisture [4, 6]. The AlN in SAD generates ammonia, which is corrosive and poses health risks ranging from respiratory irritation to burns, blindness, lung damage, or death, depending on exposure levels. Ammonia odor is detectable at five ppm and tolerable up to 100 ppm for hours. Prolonged exposure to ammonia can cause pharyngitis, sore throat, rhinitis, and other health issues, as well as mortality. At 1700 ppm, it can cause coughing, throat spasms, and edema. In addition, exposure to 2500-4500 ppm can be fatal within 30 minutes, while levels above 5000 ppm cause rapid respiratory arrest, and concentrations above 10,000 ppm can damage the skin.

Ammonia concentrations in SAD from large-scale SMEs in Jombang ranged from 130,000 to 170,000 ppm, consistent with previous studies reporting 72,000 to 182,000 ppm [11]. These findings highlight the serious health risks associated with ammonia exposure. In the air, ammonia reacts with other gases to form the harmful PM2.5 pollutant, while in water, it increases pH levels, harming aquatic life. In addition, its corrosive nature can damage metals and industrial infrastructure. Therefore, denitrification pre-treatment is essential to minimize these impacts, which can be achieved through effective humidity control, ventilation, and ammonia removal.

Effective ammonia removal focuses on the hydrolysis of AlN under controlled temperature and pH, often involving additives such as AlF_3, NaF, Na_2CO_3, or NaOH. Previous studies have shown that 96.24% ammonia removal efficiency can be achieved at 95 °C within 180 minutes using 4wt% NaOH (by SAD weight) and a L/S ratio of 6 mL/g.

On a local scale, a large-scale SME in Jombang tested an alternative ammonia reduction method by spraying SAD with water, phosphoric acid, and ammonia, supplemented with NaOH and $CaCO_3$. This technique successfully reduced the ammonia concentrations from 13.00%, 15.00%, and 17.00% to 1.67%, 2.66%, and 3.76%, with removal efficiencies of 87.17%, 82.26%, and 77.88%, respectively. Furthermore, controlling the solution volume allowed the formation of stable salts within the SAD, which could prevent the production of ammonia-contaminated wastewater.

6. Conclusions

This study optimized ammonia removal from SAD using a heat-stirred alkaline leaching process with Box-Behnken Design and Response Surface Methodology. It evaluated the effects and interactions of NaOH concentration, temperature, reaction time, and stirring speed on removal efficiency to identify optimum and sustainable operating conditions. The key findings are summarized as follows:

(1) Ammonia removal reached 98.81%, while an alternative condition achieved 98.34% with lower chemical and energy use.
(2) Temperature and reaction time were identified as the most influential individual factors enhancing ammonia hydrolysis.
(3) Interaction effects between NaOH concentration and temperature, and temperature and stirring speed were critical for maximizing removal efficiency.
(4) The optimized process enables the safe reuse of SAD as a source of alumina in cement production, supporting waste reduction, improving worker safety, and lowering environmental and health risks, thereby enhancing sustainability and economic viability.

Acknowledgments

The authors acknowledge the National Research and Innovation Agency of Indonesia (BRIN) for funding this research through the Research Organization for Life Sciences and Environment for the 2024 fiscal year. The authors also thank the

Laboratory for Advanced Characterization Physics and the Laboratory for Energy Resources, Fuel, and Environment—BRIN—for providing the laboratory facilities.

Conflicts of Interest

The authors declare no conflict of interest.

References

[1] M. Dada and P. Popoola, "Recent Advances in Joining Technologies of Aluminum Alloys: A Review," Discover Materials, vol. 4, article no. 86, 2024.

[2] S. Van den Eynde, et al., "Forecasting Global Aluminium Flows to Demonstrate the Need for Improved Sorting and Recycling Methods," Waste Management, vol. 137, pp. 231-240, 2022.

[3] International Aluminium Institute, "Primary Aluminium Production," https://international-aluminium.org/statistics/primary-aluminium-production/?publication=primary-aluminium-production, 2024.

[4] J. Liu, S. Zhang, H. Shen, B. Lou, and B. Zhang, "Recycling of Secondary Aluminum Dross to Make Alumina by Hydrometallurgy: A Review," Journal of Materials Research and Technology, vol. 32, pp. 4234-4245, 2024.

[5] H. Kvande, G. Saevarsdottir, and B. J. Welch, "Direct and Indirect CO_2 Equivalent Emissions from Primary Aluminium Production," Light Metals 2022, Springer, Cham, pp. 998-1003, 2022.

[6] G. Çil and K. Yildiz, "Evaluation of Secondary Aluminium Dross in Calcium Aluminate Cement," Materials and Technology, vol. 56, no. 5, pp. 541-546, 2022.

[7] R. Beheshti, "Sustainable Aluminium and Iron Production," Ph.D. dissertation, School of Chemical Science and Engineering, KTH Royal Institute of Technology, Stockholm, 2017.

[8] S. K. Padamata, A. Yasinskiy, and P. Polyakov, "A Review of Secondary Aluminum Production and Its Byproducts," JOM, vol. 73, pp. 2603-2614, 2021.

[9] D. Abhishek, "Thermal Plasmas for Industrial High-Temperature Processes: Modelling Study of Aluminium Smelting," Master's thesis, Nordic Master Programme in Innovative and Sustainable Energy Engineering, Aalto University, 2022.

[10] M. J. A. Mansor, et al., "Process Optimization of Alumina Extraction from Aluminium Dross Via Response Surface Methodology," Malaysian Journal of Chemistry, vol. 26, no. 6, pp. 121-315, 2024.

[11] V. Milani and G. Timelli, "Solid Salt Fluxes for Molten Aluminum Processing–A Review," Metals, vol. 13, no. 5, article no. 832, 2023.

[12] J. Liu, S. Zhang, B. Lou, and H. Shen, "Formation of Aluminum Nitride in Dross by Contact-Diffusion Reaction During Aluminum Recycling," Journal of Alloys and Compounds, vol. 1010, article no. 177432, 2025.

[13] H. L. Yang, Z. S. Li, Y. D. Ding, Q. Q. Ge, and L. Jiang, "Hydrolysis Behavior and Kinetics of AlN in Aluminum Dross During the Hydrometallurgical Process," Materials, vol. 15, no. 16, article no. 5499, 2022.

[14] A. Hafidz, "70,000 Tons of Hazardous Aluminum Dross Waste in Jombang Have Remained Unmanaged Since the 1970s," https://radarjombang.jawapos.com/nasional/665043215/70000-ton-timbunan-limbah-b3-abu-aluminium-di-jombang-belum-tertangani-sejak-tahun-1970an, 2024.

[15] Y. Li, et al., "Hazardous Characteristics and Transformation Mechanism in Hydrometallurgical Disposing Strategy of Secondary Aluminum Dross," Journal of Environmental Chemical Engineering, vol. 9, no. 6, article no. 106470, 2021.

[16] X. Zhu, J. Yang, Y. Yang, Q. Huang, and T. Liu, "Pyrometallurgical Process and Multipollutant Co-Conversion for Secondary Aluminum Dross: A Review," Journal of Materials Research and Technology, vol. 21, pp. 1196-1211, 2022.

[17] Q. Guo, et al., "Enhanced Hydrolysis of Aluminum Nitride from Secondary Aluminum Dross Through Combination of Wet-Stirred Milling and Alkaline Leaching," Waste and Biomass Valorization, vol. 14, no. 12, pp. 4257-4268, 2023.

[18] Indonesian Geospatial Information Agency, "Administrative Area Boundary," https://geoservices.big.go.id/portal/apps/webappviewer/index.html?id=49bda2cefd3f4b92aa726300bcdb40f7, accessed in 2025.

[19] Q. Jiang and B. Lee, "Optimizing Wet Hydrolysis for Nitrogen Removal and Alumina Recovery from Secondary Aluminium Dross," Sustainability, vol. 16, no. 13, article no. 5312, 2024.

[20] D. C. Montgomery, Design and Analysis of Experiments, 10th ed., Hoboken: John Wiley & Sons, 2019.

[21] H. Lv, H. Zhao, Z. Zuo, R. Li, and F. Liu, "A Thermodynamic and Kinetic Study of Catalyzed Hydrolysis of Aluminum Nitride in Secondary Aluminum Dross," Journal of Materials Research and Technology, vol. 9, no. 5, pp. 9735-9745, 2020.

[22] C.Wang, et al., "Mechanism of the Denitrification of Secondary Aluminum Dross During Water Leaching with Delayed Addition of a Low Dosage of Sodium Hydroxide," Hydrometallurgy, vol. 226, article no. 106318, 2024.
[23] Y. Zhang, Z. Guo, Z. Han, and X. Xiao, "Feasibility of Aluminium Recovery and $MgAl_2O_4$ Spinel Synthesis from Secondary Aluminium Dross," International Journal of Minerals, Metallurgy, and Materials, vol. 26, pp. 309-318, 2019.
[24] W. C. Lips, E. B. Braun-Howland, and T. E. Baxter, Standard Methods for the Examination of Water and Wastewater, 23rd ed., American Water Works Association, 2023.
[25] A. Zezulová, T. Staněk, and T. Opravil, "The Influence of Barium Sulphate and Barium Carbonate on the Portland Cement," Procedia Engineering, vol. 151, pp. 42-49, 2016.
[26] T. Suwan, et al., "Influence of Ammonia-Contaminated Fly Ash from Selective Catalytic Reduction Process on the Properties of Portland-Fly Ash Blended Cement and Geopolymer Composites," Case Studies in Construction Materials, vol. 22, article no. e04563, 2025.
[27] P. Puksisuwan, P. Laoratanakul, and B. Cherdhirunkorn, "Utilization of Aluminium Dross as a Main Raw Material for Synthesis of Geopolymer," Journal of Metals, Materials, and Minerals, vol. 27, no. 2, pp. 35-42, 2017.
[28] M. Gallardo, J. M. Almanza, D. A. Cortés, J. C. Escobedo, and J. I. Escalante-García, "Synthesis and Mechanical Properties of a Calcium Sulphoaluminate Cement Made of Industrial Wastes," Materiales de Construcción, vol. 64, no. 315, article no. e023, 2014.

Appendix

Table A1 Top 15 experimental runs with the highest desirability scores for ammonia removal optimization

No.	NaOH concentration (%)	Temperature (°C)	Reaction time (Minute)	Stirring (rpm)	Ammonia removal (%)
1	5.30	94.19	239.49	398.49	98.81
2	6.39	94.29	219.23	352.26	98.60
3	6.24	94.62	231.99	292.72	98.47
4	6.38	94.88	166.86	351.44	98.35
5	2.90	94.22	217.62	399.70	98.34
6	4.90	93.90	217.77	308.58	98.30
7	6.59	94.70	196.62	294.88	98.27
8	5.15	94.66	153.35	364.04	98.27
9	6.69	94.30	170.90	347.26	98.27
10	2.98	92.92	228.19	391.97	98.19
11	4.95	92.40	148.15	398.55	98.16
12	5.19	94.94	217.58	236.47	98.15
13	3.50	95.00	135.00	400.00	98.11
14	6.03	94.78	235.96	117.75	98.10
15	4.17	91.85	211.26	352.63	98.10